Electricity-assisted thermochemical sorption system for seasonal solar energy storage

Zhiwei Ma, Huashan Bao*, Anthony Paul Roskilly

Department of Engineering, Durham University, Durham, UK, DH1 3LE

*Corresponding author: Dr Huashan Bao, Tel: +44 (0) 0191 334 1706; E-mail address: huashan.bao@durham.ac.uk.

Abstract

The present paper investigated the seasonal solar thermal energy storage (SSTES) using solid-gas thermochemical sorption technology that has inherently combined function of heat pump and energy storage. The thermochemical reactions that can discharge heat at a higher temperature usually requires a relatively higher desorption temperature during charging process, which could be problematic to efficiently recover solar energy in high-latitude regions like the UK when using the most mature and economic solar thermal collector (flat-plate or evacuated tube type). The present work studied two hybrid concepts where an electric-driven compressor or an electric heater was introduced to supplement the thermochemical desorption process in terms of pressure rise and temperature lift, respectively, when the available solar heat is not sufficiently high. As $SrCl_2$-8/1NH_3 chemisorption was selected from 230 ammonia chemisorption reactions due to its suitable adsorption/desorption temperature and large energy storage density, the performance of two hybrid systems using $SrCl_2$-8/1NH_3 chemisorption were evaluated and compared to determine the more efficient solution. The results revealed that the hybrid thermochemical sorption with a compressor substantially improved the storage capacity compared to that with electric heater. With a compression ratio of 4, the SSTES system with 20 m^2 solar collector under the weather condition of Newcastle upon Tyne can store 3226.8 kWh chemisorption heat by charging 4465.4 kWh solar heat and 848.2 kWh electricity, indicating 60.7% of the charged energy was non-loss; the corresponding energy density based on the overall system volume is 147.3 kWh/m^3. Because of using the renewable solar heat and low carbon intensity electricity in summer, the proposed hybrid SSTES system has noteworthy reduction on carbon emission compared to gas boiler and conventional heat pump.

Keywords: Seasonal storage; Solar energy; Thermochemical sorption; Electric heater; Compressor; Hybrid system

Nomenclature

Cp	specific heat (J/(kg K))
E	electricity (J)
k	adiabatic index (-)
ΔH_0	enthalpy change (J/mol)
$\dot{m}$	mass flow rate (kg/s)
M	molar mass (kg/mol)
P	pressure (Pa)
Q	heat (kWh)
r_{com}	compression ratio (-)
R	gas constant (J/(mol K))
R_g	specific gas constant (J/(mol K))
S	specific adsorption capacity (kg/kg)
ΔS_0	entropy change (J/(mol K))
T	temperature (K)
U	energy density (kWh/m^3)
V	volume (m^3)
$\dot{W}$	power (W)
x	mole number (mol)
Greeks	
γ	stoichiometric coefficient (-)
η	efficiency (-)
ρ	density (kg/m^3)
η	efficiency (-)
Subscripts	

ads	adsorption
amb	ambient
che	chemisorption
com	compressor
des	desorption
E	electricity
max	maximum
min	minimum
NH_3	ammonia
nl	non-loss
s	salt
sw	switch on
sys	system
tot	total

1 Introduction

Space heating and hot water heating consumes about 46143 thousand tonnes of oil equivalent (ktoe) across domestic, industry and service in 2017 in the UK, which is about 56.5% of the total energy consumed by these three energy sectors, and about 32.7% of the total energy consumption by the entire UK economy [1]. Gas is the main energy source for space and hot water heating in the UK, which accounts for about 80%. To reduce the CO_2 emission and improve the system energy efficiency and security, it is urgent to develop low carbon heating technologies and allow more penetration of renewable energy in space and hot water heating. Beside the active heating technologies, thermal energy storage is significantly important for the future of low carbon heating. The seasonal solar thermal energy storage (SSTES) is aimed to achieve 'free' heating by storing solar heat in summer and releasing heat in winter [2]. One of the key performance indicator of a SSTES is the volumetric energy density which determines the system volume. Some pioneer projects conducted between 1996-2008 using water as a SSTES material in Germany [3] at community scale, and the storage volume ranging from several to more than 50 thousands of cubic meters. Some of these were combined with heat pump technology. The operational results revealed large heat loss over time and low

energy storage density (<50 kWh/m^3). Using latent heat storage marginally increases the energy storage density, the theoretical value can achieve 60 kWh/m^3 (Triacontane, 250 kJ/kg latent heat, 50 °C temperature difference, 25% heat loss), which is still not high enough for a desirable compact system and high heat loss remains unresolved [4]. Thermochemical energy storage has been recognised as one of the most promising technologies for SSTES due to the large storage density and near-zero energy loss [5-7]. Thermochemical sorption technology has been widely studied and demonstrated in the area of decarbonisation of heating and cooling and can be easily scaled up and applied to SSTES systems [8-10]. Thermochemical heat pump outperforms the conventional heat pump in two points, (1) thermochemical heat pump is a thermal-driven heat pump with zero-emission as it enables effective utilisation of low grade heat such as solar heat and geothermal energy or industrial waste heat. On the contrast, widespread use of the conventional heat pump could pose significant challenges to the grid, as it increases peak electricity demand in the winter (a million extra heat pumps could add 1.5 GW to peak demand) [11, 12]. (2) Thermo-chemical heat pump uses environmental-friendly refrigerant instead of those HFCs with Global Warming Potential. Hence, the SSTES based on thermochemical sorption technology is a promising solution for clean growth and sustainable society.

Ma et al. [13, 14] evaluated the SSTES system using ammonia-based thermochemical sorption cycle, and concluded that there was a dilemma to select suitable adsorbents: the usage of middle temperature adsorbents could meet the heating requirement through radiators system in winter but also requires relatively higher regeneration (energy charging) temperature in summer, which makes it problematic to recover solar energy in high-latitude regions like the UK, i.e. limited solar heat can be stored during summer; the usage of low temperature salt allowed relatively larger amount of low temperature solar heat to be stored but the heat output during adsorption (energy discharging) process in winter was at comparatively lower temperature, thus low temperature indoor heating facilities (25-35 °C) such as underfloor heating or convector heating must be used. The authors recommended the use of $BaCl_2$-0/8NH_3 chemisorption within a 45.2 m^3 SSTES system powered by 30.5 m^2 solar collector, which can cover about 57.4% heating demand of a house by means of low temperature heating systems, under the UK climatic conditions. Li et al. [15, 16] recommended using two-stage thermochemical sorption system which employed two sets of ammonia chemisorption units including reactor and condenser/evaporator to achieve sufficiently high temperature heat discharging. In this instance, during the cold winter, the adsorption heat of the first stage cycle was used as desorption heat for

the second stage cycle to realise two steps of temperature lifts. Hence, the storage system could release satisfactory heating for a wide range of atmospheric conditions (from −30 °C to 15 °C). The shortcoming of this mothed was the low energy storage density and complicated system control. Jiang et al. [17] experimentally studied $MnCl_2$-$CaCl_2$ resorption as the SSTES process, the required charging temperature was at 150 °C and the discharging temperature was only 30 °C when the atmospheric temperature at 15 °C. The authors further proposed using a compressor to boost the desorption pressure of the $CaCl_2$ ammine during the discharging process to a higher level so as to achieve a higher adsorption temperature of the $MnCl_2$ ammine. This method faced the challenge of identifying a suitable compressor that worked at vacuum condition, low temperature and low density of ammonia vapour. Moreover, using the electric-driven compressor during discharging process would still put pressure on the main grid during the peak demand period.

To address the foregoing dilemma stemmed in the thermodynamic properties of thermochemical sorption when applied to SSTES for domestic heating, the current paper studied two types of hybrid electricity-assisted thermochemical sorption systems, which can provide satisfactory heating in winter through commonly used radiator heating system. Both studied systems integrate thermochemical sorption with one electrical element to enhance the system capability and flexibility due to one more degree of freedom for operation. They also increase integration of renewable energy sources as both renewable thermal and electrical energy is recovered and utilised when, for example, coupling with a solar photovoltaic-thermal (PV/T) collector as solar energy undergoes both photo-thermal and photo-electric conversion. Instead of putting extra peak-demand pressure on the main grid in winter, these two studied systems only consume electricity to assist endothermic desorption process in summer when the electricity is cleaner and cheaper, i.e. electrifying part of heat load and seasonally shifting energy load (both heat and electricity).

According to the mono-variant thermodynamic equilibrium of chemisorption, which can be represented either by temperature or pressure, there are obviously two approaches to implement the electricity-assisted thermochemical sorption cycle, (1) the first one is the most straightforward method of directly changing the temperature condition, using an electric-heater to lift up the temperature level of the supplied heat to meet the desorption requirement; (2) the second one is associated with direct pressure change, using an compressor to electrically pressurising the process. These two hybrid systems were analysed and compared

for the first time in the present work, more insights for optimal operation and system design was also provided and discussed.

2 System description and salt selection

2.1 Electricity-assisted thermochemical sorption SSTES systems

The schematic of two types of electricity-assisted thermochemical sorption SSTES systems and the corresponding thermodynamic *P-T* processes are shown in Figure 1. Each system layout is consisted of a flat-plate solar collector, an ammonia chemisorption reactor, a condenser/evaporator, an electric heater or a compressor.

The chemisorption reactor was designed as a shell-and-finned tubes heat exchanger, the adsorbent material is packed outside each tube module and in the space of the fin gaps while the heat transfer fluid (HTF) flows inside each tube.

During the heat charging process, the HTF, e.g. water, is heated by solar collector and flows to the chemisorption reactor to desorb the ammonia that thereby condenses in the condenser at the ambient temperature. The finned tubes inside the reactor can be heated at the same time, or group by group in the manner of series connection, to have better heating performance. If the HTF has relatively low temperature at the outlet of solar collector, which does not reach the desorption temperature level, an electric heater is used to elevate the HTF temperature, as shown in Figure 1(a); alternatively, as shown in Figure 1(b), a compressor is used and installed in between the reactor and the condenser to pressurise the desorbed low pressure ammonia so as to condense the ammonia at ambient temperature. In this instance, the desorption always can occur if required even though the solar radiation is insufficient to generate high temperature hot water. The electricity input could be from solar PV panel or PV/T collector or from the grid in summer.

During the heat discharging process, the liquid ammonia inside the evaporator evaporates at the ambient temperature while the adsorbent adsorbs ammonia and releases considerable amount of adsorption heat. The returned water from the space and water heating system flows into the chemisorption reactor firstly to absorb the released adsorption heat as much as possible; afterwards, the heated water flows to the solar collector to be further heated if possible, depending on the availability of solar energy and the ambient temperature. Although in the system design as shown in Figure 1(c), an electric heater (or other heating equipment) is

considered as back-up in case of extreme weather conditions, the adsorbent was carefully selected to avoid electricity consumption at all in winter.

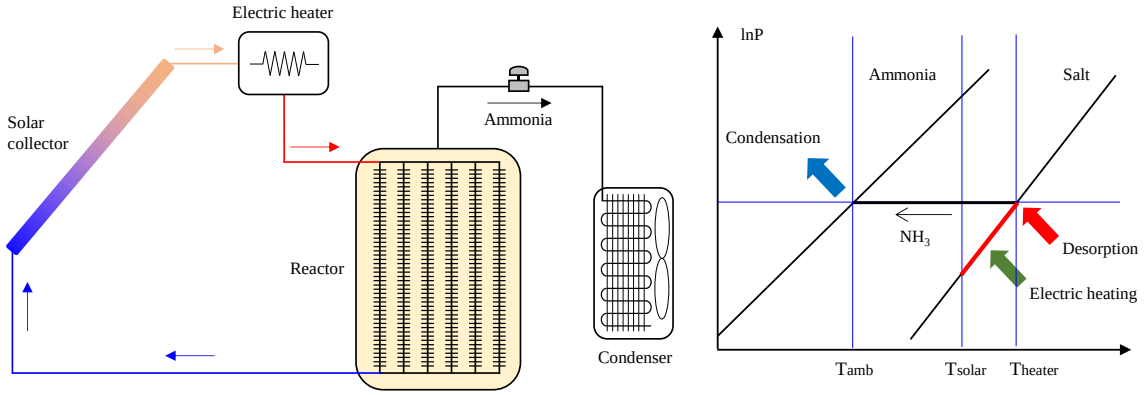

(a)

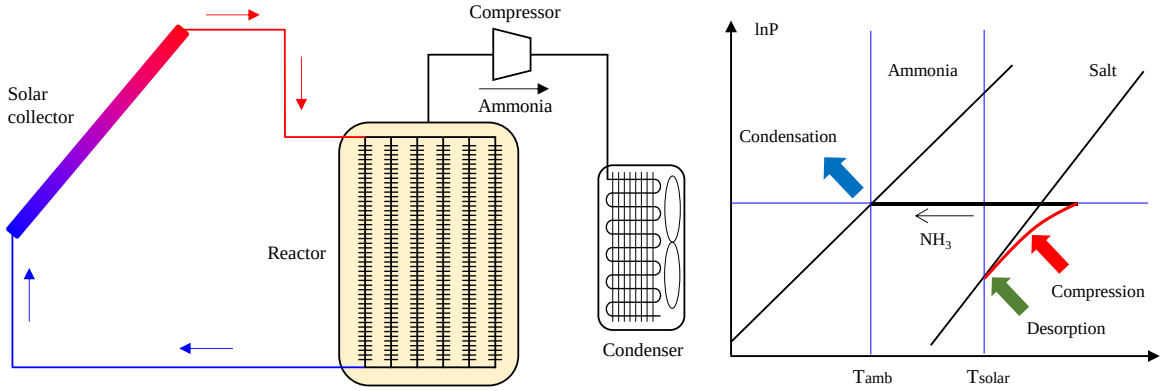

(b)

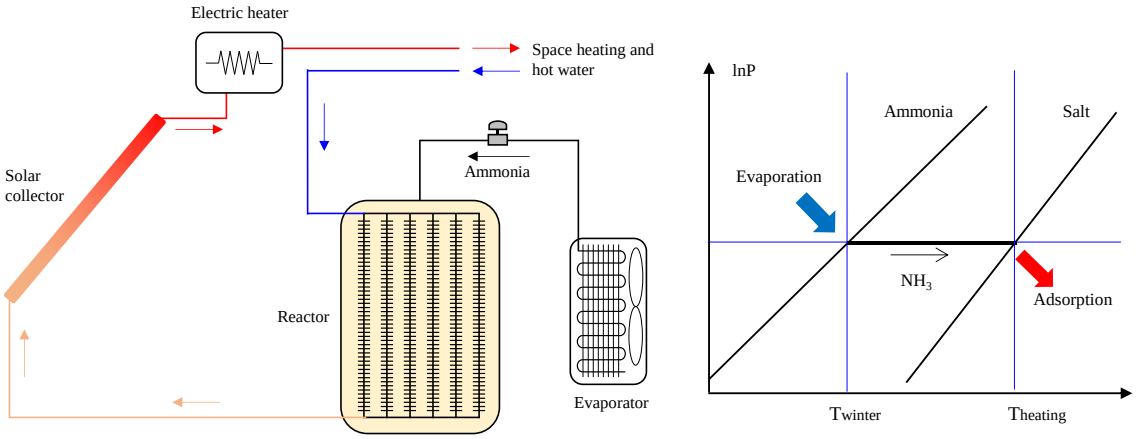

(c)

Figure 1 Schematic diagram of ammonia chemisorption SSTES system and corresponding thermodynamic *P-T* process, (a) charging process with electric-heating process; (b) charging process with electric-compression; (c) discharging process.

2.2 Salt selection

More than 230 ammonia chemisorption reactions with more than 80 salts were reviewed and analysed to sift out the suitable reaction for the studied SSTES system [18-21]. There are three criteria for selection:

- The salt should be safe.
- The specific adsorption capacity and the volumetric energy density are high;
- The thermodynamic properties match with the operating conditions, i.e. desorption temperature is achievable by flat-plate collectors, and adsorption temperature is higher than the desired temperature level of space heating and hot water heating through the commonly used radiators.

The specific adsorption capacity (the mass amount of ammonia can be adsorbed by unit mass of adsorbent, kg/kg) and volumetric energy density (kWh/m^3) of the material were calculated based on the following equations, respectively:

$$S = \gamma \frac{M_{\mathrm{NH3}}}{M_{\mathrm{s}}} \quad (1)$$

$$U_{\mathrm{m}} = \Delta H_0 \gamma \frac{\rho_{\mathrm{s}}}{3.6\times10^6 M_{\mathrm{s}}} \quad (2)$$

where ρ_{s} is the salt packing density, M_{s} is the salt molar mass, M_{NH3} is the ammonia molar mass, γ is the stoichiometric coefficient of the reaction. The results are listed in Table 1 with 16 shortlisted reactions, as the salt packing density was 450 kg/m^3.

Hourly temperatures in Newcastle upon Tyne from the weather software Meteonorm (mean value between year 1991 and year 2010) were used for analysis. The maximum and minimum temperatures were 26.3 °C and −1.1 °C from April to September, and 18.9 °C and −4.8 °C in winter from October to March, which were used to calculate the corresponding maximum/minimum equilibrium pressure of ammonia condensation/evaporation, thereafter the required desorption temperature in charging process in summer and the adsorption temperature in discharging process in winter were derived based on the following equation while considering 1.0 bar equilibrium pressure drop (P_{NH3} − 1 bar for adsorption and P_{NH3} + 1 bar for desorption)

$$\ln P = -\frac{\Delta H_0}{RT} + \frac{\Delta S_0}{R} \quad (3)$$

The maximum and minimum desorption and adsorption temperatures required of different adsorbents are presented in Table 1. $CaCl_2.4/8NH_3$, $BaBr_2.4/8NH_3$, $NaI.0/4.5NH_3$ and $SrCl_2.1/8NH_3$, highlighted with grey-

colour background, were short-listed with suitable thermodynamic properties for the studied SSTES system, among them $SrCl_2.1/8NH_3$ has the highest specific adsorption capacity and energy density, hence this reaction was eventually selected by the current study to explore the feasibility of the proposed hybrid SSTES system.

Because of its preferable thermodynamic properties and sorption capability, the $SrCl_2$ ($1/8NH_3$) reaction has been recently studied for different applications. Johannessen et al. [22] designed and studied an ammonia storage and delivery system (ASDS/AdAmmine) based on chemisorption cycle that uses $SrCl_2$ ammine compound. The designed $SrCl_2$ sorption system had an ammonia storage capacity more than twice that of urea-SCR system; additionally, with a dosing temperature at 100 °C it reduced tailpipe NO_x emission by half of that by urea-SCR system dosing from 180 °C. Bao et al. [23] analysed and evaluated the low-grade-heat (60 °C ~ 180 °C)-driven chemisorption power adsorption cycles that used two different salt ammines or two identical salt ammines as a working pair. Compared to other studied salt ammines ($MnCl_2$, $BaCl_2$, NaBr), the chemisorption power generation cycle of the $SrCl_2$–$SrCl_2$ pair had the highest value of energy density, the relatively higher work output per mass unit of ammonia, and the higher ammonia uptakes per mass unit of metallic salt. Wu et al. [24] reported their experimental investigation on a thermochemical sorption refrigeration prototype using $SrCl_2$-NH_3 working pair, as it was powered by thermal energy below 100 °C for the refrigeration from 5 to −15 °C. The achieved COP was 0.13~0.22 and the SCP ranged from 115 to 185 W/kg when the global conversion reached about 42%. Thinsurat et al. [25] studied a seasonal solar thermal storage system that integrated the chemisorption cycle of the $SrCl_2$–NH_3 reaction with the solar Photovoltaic/Thermal (PV/T) collector. It was demonstrated that the $SrCl_2$–NH_3 thermochemical sorption system coupled with a 26 m^2 air-gap PV/T collector could fully satisfy the hot water demand all year around and half of the annual electricity consumption for a single household in Newcastle upon Tyne. Huang et al. [26] and Yuan et al. [27] developed global kinetic models and identified optimal thermal and kinetic parameters for the $SrCl_2$ ($1/8NH_3$) reaction.

Table 1 Desorption and adsorption temperatures and volumetric energy densities of screened ammonia chemisorption reactions.

Salt	Higher NH_3 number	Lower NH_3 number	S	ΔH_0	ΔS_0 [a]	Ref	$T_{des,\,max}$	$T_{des,\,min}$	$T_{ads,\,max}$	$T_{ads,\,min}$	U_m [b]
	-	-	kg/kg	J/mol	J/(mol K)		°C	°C	°C	°C	(kWh/m^3)
$PbCl_2$	8	3.25	0.290	35300	132	[19]	42.50	24.84	32.17	11.13	75.37
KI	4	0	0.410	29500	113.1	[18]	44.29	23.15	31.86	7.07	88.85
NaBr	5.25	0	0.867	30491	208.8	[20]	55.04	33.18	42.19	16.55	194.47
$BaCl_2$	8	0	0.653	37665	227.25	[21]	65.09	46.08	53.96	31.34	180.88
$CaCl_2$	8	4	0.613	41013	230.3	[21]	85.33	65.70	73.85	50.43	184.78
$BaBr_2$	8	4	0.229	41600	134.5	[18]	90.70	70.76	79.04	55.25	70.00
NaI	4.5	0	0.510	39000	127.2	[18]	91.23	69.97	78.78	53.56	146.36
$SrCl_2$	8	1	0.751	41431	228.8	[21]	93.80	73.45	81.89	57.64	228.68
$SrBr_2$	8	2	0.412	46900	138	[19]	124.88	103.67	112.49	87.14	142.16
$MnCl_2$	6	2	0.540	47416	228.07	[21]	149.54	125.95	135.74	107.64	188.39
$CaBr_2$	6	2	0.340	50200	138.7	[18]	150.37	127.93	137.26	110.43	125.57
$FeCl_2$	6	2	0.536	49700	128	[19]	187.76	161.06	172.12	140.42	196.05
$NiSO_4$	6	2	0.439	59500	146.1	[18]	199.33	175.70	185.54	157.16	192.25
$CoCl_2$	6	2	0.524	53968	228.01	[21]	208.20	181.33	192.48	160.47	207.83
$MgCl_2$	6	2	0.714	55660	230.63	[21]	211.96	185.46	196.46	164.85	292.30
$NiCl_2$	6	2	0.525	59217	227.75	[21]	256.25	226.62	238.92	203.64	228.46

[a] The calculated pressure using ΔS_0 given by [18] and [19] has the unit of Pa, while others are based on the unit of bar; [b] assuming a 450 kg/m^3 salt packing density

3 Analysis methods

3.1 Available solar heat and ammonia chemisorption simulation

The solar radiation data of Newcastle upon Tyne provided by the weather software Meteonorm was used to determine the useful solar heat production by a 20 m^2 flat-plate solar collector, as the value of 20 m^2 represents the average roof area of domestic dwellings in the UK [28]. The calculation method of the available solar heat and the modelling and simulation of the chemisorption reactor have been reported in our previous work [14].

208 Some parameters of each modular finned tube that was packed with adsorbents and contained in the shell
209 reactor are presented in Table 2.
210
211 Table 2 Parameters of the modular chemisorption finned tube.

Parameters	Values
Tube ID (mm)	20
Tube OD (mm)	24
Fin diameter (mm)	150
Fin thickness (mm)	1
Fin number (-)	200
Length (mm)	2200
Adsorbent bulk density (kg/m^3)	600
Adsorbent mass (kg)	20.66
Adsorbent bulk volume (m^3)	0.0344
Module volume (m^3)	0.0389
Expanded graphite mass ratio (-)	0.25
Degree of reaction conversion range (-)	0.05-0.95

212
213 3.2 Electric heater and compressor control strategies
214 The goal of the control strategy in the present work is to maximise the utilisation of solar heat and avoid
215 electricity consumption as much as possible. It should be noted that if the studied SSTES system is
216 integrated with solar PV/T panel, because both heat and electricity is from solar, the control strategy should
217 try to balance these two types of energy products (i.e. inputs for SSTES system) and maximise the overall
218 solar energy conversion and utilisation.
219 For the system equipped with electric heater (SSTES-H), a temperature threshold for activating the electric
220 heater is defined as a switch-on temperature (T_{sw}). That means there are three scenarios of electric heater
221 operation:
222 (1) If the solar heat temperature (i.e. HTF temperature) is higher than the equilibrium desorption temperature
223 and provides 5 ºC temperature equilibrium drop, there is no need of extra electricity input;

(2) Except the conditions in case 1, when the temperature of HTF at the outlet of solar collector is higher than the switch on temperature (T_{sw}), the electric heater switches on. Thus, the HTF is further heated by the electric heater and maintained at 5 °C higher than T_{des}.

(3) If the HTF temperature was lower than the T_{sw}, the electric heater is off to avoid excessive electricity consumption, in this instance the HTF heats up the reactor without triggering desorption, i.e. no energy charging to the storage system.

Therefore the energy consumed by the electric heater was calculated only in the second scenario based on the following equation

$$\dot{W}_{E} = \dot{m} c_p (T_{des} + 5 - T_{sw}) \quad (4)$$

For the system that uses compressor (SSTES-C), a compression ratio was pre-defined in the range of 2-8. Similarly to the first and third scenarios of using electric heater, the compressor was by-passed when the HTF temperature at the outlet of solar collector was higher than T_{des} or too low; otherwise, the compressor with was switched on to pressurise the desorbed ammonia for condensation, therefore the desorption at lower constraint temperature could be enabled by the compressor (P_{des}/r_{com}). The consumed compression work was calculated by the following equation

$$\dot{W}_{com} = \dot{m} \frac{k}{k-1} R_g T_{des} \left(1 - r_{com}^{\frac{k-1}{k}}\right) / \eta_{com} \quad (5)$$

where k is the adiabatic index of ammonia, a value of 1.312 was used in the current study, the inlet ammonia temperature was assumed to be equal to the desorption temperature, η_{com} is the efficiency of the used compressor and was set at 0.8.

3.3 System volume, chemisorption heat storage density and storage efficiency

The system volume was calculated based on the number of the modular finned-tubes that underwent desorption during the charging process, as each module occupied about 0.0389 m^3 including the finned tube, the adsorbent and the HTF, and the total volume of these modules was considered taking 80% of the total volume of the overall system as a whole for a compact design.

The volumetric energy storage density discussed in this study was based on the ‘non-loss’ chemisorption heat as shown in Eq. (6), and the ‘non-loss’ chemisorption heat is represented by the reaction enthalpy associated with the pure desorption/adsorption that is stored as chemical potential energy, as expressed in Eq.

(7) where the ΔH_r is the reaction enthalpy per mole of the reacted ammonia and the x is the mole number. The storage efficiency in Eq. (8) is the ratio of the stored chemical potential energy, i.e. 'non-loss' chemisorption heat, to the total charged energy including solar heat and electricity input.

$$U_{\text{sys, nl}} = \frac{Q_{\text{che}}}{V_{\text{tot}}} \tag{6}$$

$$Q_{\text{che}} = \Delta H_r \cdot x \tag{7}$$

$$\eta_{\text{store}} = \frac{Q_{\text{che}}}{Q_{\text{solar}} + E_{\text{in}}} \tag{8}$$

4 Results and discussion

During the thermal charging process, the consumed thermal energy was divided into two parts, one was consumed for sensible heat as the temperature of the reactor and adsorbent material was increased from ambient temperature level up to a certain temperature in order to initiate desorption, while the other part is the chemisorption heat (reaction enthalpy), only this part is 'non-loss' as the heat is stored in the form of chemical potential. Therefore the following discussion focuses on the amount of chemisorption heat that can be stored and the corresponding solar heat input and electricity input.

4.1 System with electric heater (SSTES-H)

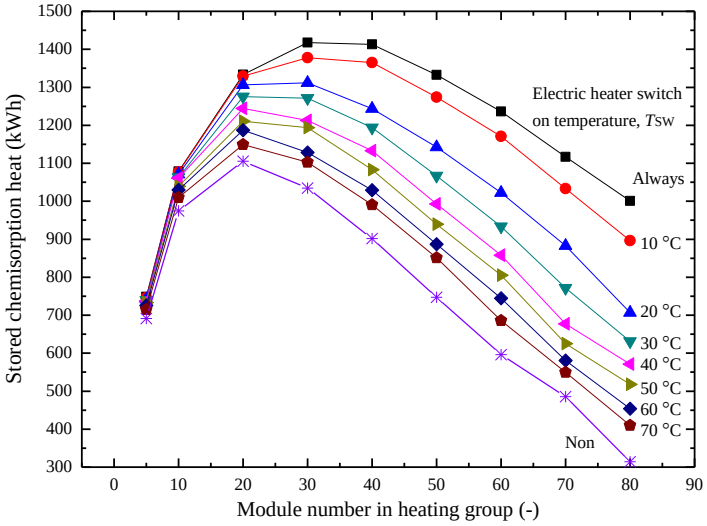

Figure 2 Stored chemisorption heat of SSTES-H, as the functions of module number in heating group and electric heater switch on temperature.

The variation profile of the stored chemisorption heat as the function of the number of the finned-tube modular tubes in heating group is shown in Figure 2. There existed an optimal module number in heating group, which was also found in the previous study [14]. More modular tubes being heated at the same time allowed more adsorbent material getting involved in the charging process at the same time; however, with the provided solar radiation, this led to the less mass flow rate of HTF through each modular tube, and the slower progression of the reaction conversion for each day time. In order to complete the reaction, each module had to take longer time and experience more rounds of temperature swing between ambient temperature and desorption temperature as the alternation of day and night. That indicates more heat input was consumed for sensible heat but less for the chemisorption heat. As shown in the figure, for the cases when the electric heat was always on or with the T_{SW} at 10 °C and 20 °C, the optimal module number is 30; while for the other cases including the case of no electric heater, the optimal module number is 20. Detailed discussion about the optimal module number can be seen in previous work [14]. The peak values of the storage capacity of these curves are 1105-1418 kWh, and it is apparent to see the usage of electric heater helping store more chemisorption heat.

Figure 3 shows the stored chemisorption heat by using the optimal module number in heating group and the correspondingly charged solar heat and electricity. When there was no electric heater, the system used 2383 kWh solar heat, but only about 46% of this heat was used as chemisorption heat that was persistent through the seasonal storage process. Using a lower "switch on" temperature of electric heater (T_{SW}), the system tended to consume more electricity in the charging process, and the storage efficiency (the ratio of the stored non-loss energy to the total charged energy) was around 38-39% when the electric heater is always on or T_{SW}=10 °C~20 °C; the storage efficiency increased up to 46-47% once the T_{SW} was no lower than 30 °C, as shown in Figure 3(a). A jump appears on the storage efficiency curve between 20 and 30 °C of the switch-on temperature, because there exists a critical point of the switch-on temperature to prevent inefficient operation. When the solar radiation is low, if the inlet temperature of HTF (return from reactors) is high and the temperature difference between the HTF and the ambient temperature is big, the solar collector could have a negative thermal efficiency as the heat it generated cannot set off the heat loss on its surface. The simulation found a critical switch-on temperature point between 20 and 30 °C for the storage efficiency under the weather condition of Newcastle upon Tyne. If the switch-on temperature is set beyond this critical

point, the abovementioned scenario with negative thermal efficiency can be completely avoided. This leads to the spike improvement in the storage efficiency of the system.

Nevertheless, it was found that using electric heater seemed not a good choice from the view point of energy conversion efficiency, for example in Figure 3(a), when T_{SW} reduced from 70 °C to 60 °C, about 200 kWh more electricity was consumed to only allow 38 kWh more chemisorption heat stored. A normal electric heater can achieve almost 100% efficiency, but the mean value of the ratio of the increased chemisorption heat stored to the extra electricity consumption is only around 12% (Figure 3(b)). That means the energy loss in the system operation is about 88%, which fails to justify the effort of energy storage and seasonal load shifting. The electricity was expected to be used as a supplementary energy source while the solar irradiation was not strong enough to supply chemisorption heat; however, when the electric heater was switched on, the heater not only had to supply the sensible heat of the adsorbent/reactor, i.e. lifting the temperature up to the desorption temperature, but also to supply the desorption heat. Therefore, the electricity became the major energy source since the desorption heat was much larger than the sensible heat. Thus it is believed that it is not wise to consume electricity through electric heater.

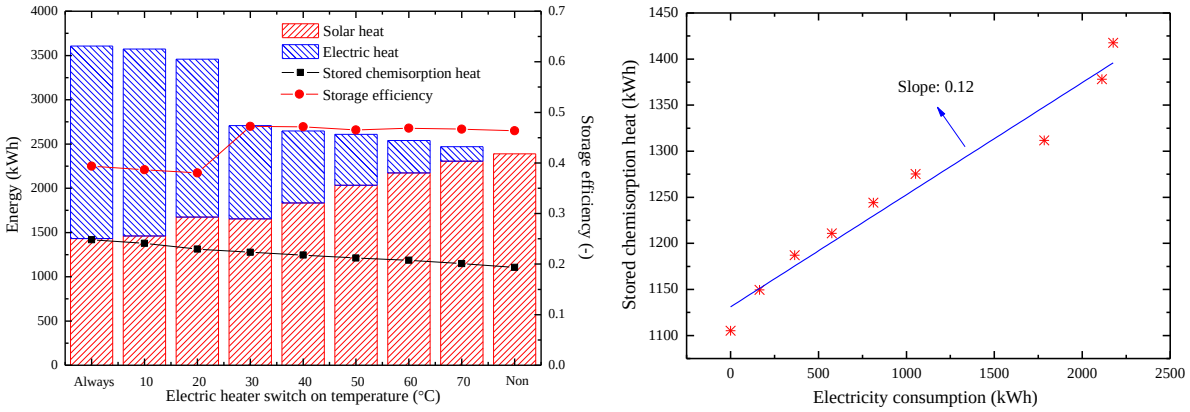

(a) (b)

Figure 3 (a) Energy and storage efficiency; (b) stored chemisorption heat *vs* electricity consumption, of SSTES-H system.

4.2 System with compressor (SSTES-C)

Figure 4 shows the variations of the stored chemisorption heat as the function of module number in heating group of the SSTES-C using different compression ratios. Similarly to the SSTES-H cases, the optimal

module number in heating group was around 20-30; nevertheless, the maximum amount of the chemisorption heat that can be stored was much larger than that of the SSTES-H, which increased from 1105 kWh in the no-compression case to 4721 kWh when using a compression ratio of 8. That is 4.3 folds increase with only 1944 kWh extra electricity consumption, because the recovered solar heat is increased by 2.46 times.

More importantly, the usage of compressor allowed majority of the heating, including the sensible heat and desorption heat, was satisfied by low grade solar heat; meanwhile only 11-26% of the total energy input is the higher quality energy, electricity, which was applied to pressurise the desorbed ammonia vapour. This achieved the rational allocation of energy sources. As shown in Figure 5, the stored heat and the charged solar heat all tangibly increases as the increase of compression ratio of the compressor. The mean ratio of the increased stored heat to the extra electricity consumption was around 1.88, nearly double the efficiency of the conventional electric heating, indicating the usage of compressor improved the storage capacity and energy utilisation efficiency. The storage efficiency of SSTES-C system generally increases from about 46% for no compression to 58-63% for using compression ratio of 2-8.

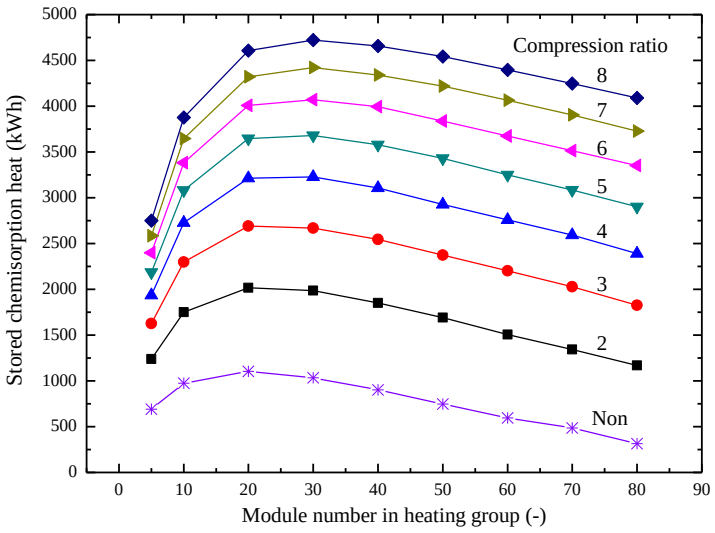

Figure 4 Stored chemisorption heat of SSTES-C system, as the functions of module number in heating group and compression ratio.

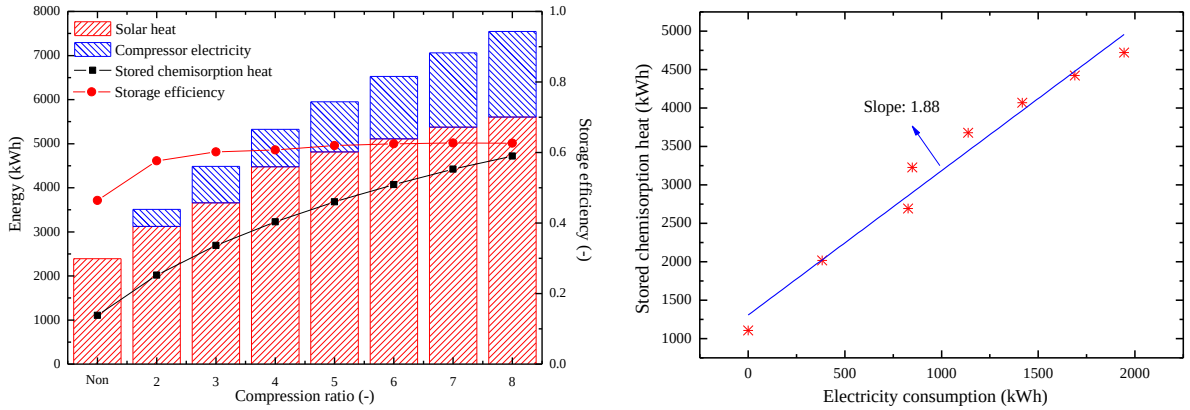

Figure 5 (a) Energy and storage efficiency; (b) stored chemisorption heat *vs* electricity consumption, of SSTES-C system.

The system volume and chemisorption heat storage density are shown in Figure 6. As the increase of compression ratio, the stored heat increased from 1105 kWh to 4721 kWh, and the corresponding required system volume was increased from about 7.5 m^3 to 32 m^3 with the storage density around 147-148 kWh/m^3. It should be noted that this storage density is at the system level and is about 64-65% of the material-based energy density which is 228.68 kWh/m^3 for $SrCl_2$-1/8NH_3 chemisorption with 450 kg/m^3 packed density of the adsorbent salt. The deduction is caused by the sensible heat loss and volumetric occupancy of fin-tubes, HTF and reactor.

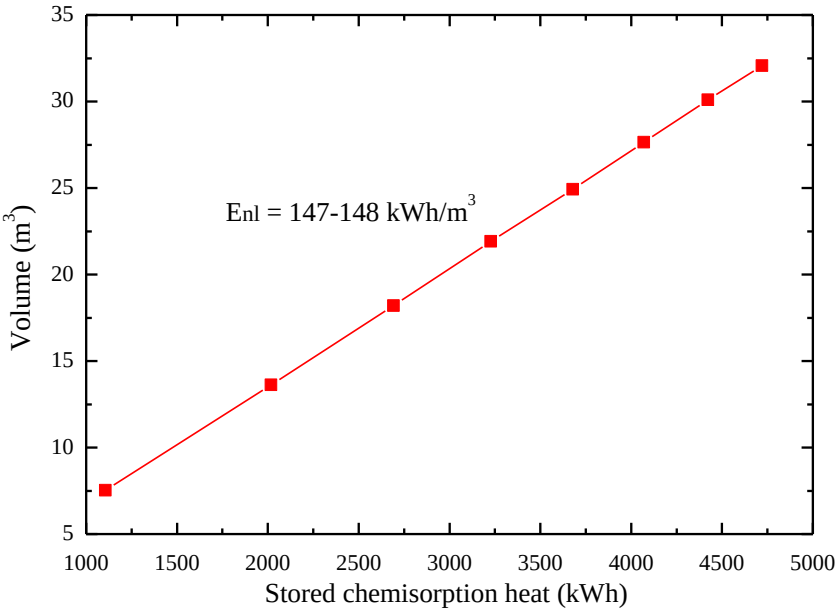

Figure 6 System volume vs the stored chemisorption heat of SSTES-C system.

As reported in literature [29] based on the statistic data of 52 UK households, the average annual heating demand per household was about 2135 kWh. This average heating demand can be satisfied with a 100% solar fraction by an SSTES-C system with a compression ratio of 3, about 14.5 m^3 storage system and 15.9 m^2 solar collector,. One of the studied 52 households had the largest heating demand of nearly 14,000 kWh heating per year. For such an untypical example, certainly a bigger solar collector and a larger storage system would be required to achieve the goal of 100% solar fraction. With the consideration of the limited roof area for solar collector installation and the limited space allowed for storage system, an SSTES-C system with a compression ratio of 5, about 37.9 m^3 storage system and 30.4 m^2 solar collector, is competent to cover 40% of the heating demand, which still indicates considerable savings of energy bill as the price of electricity and natural gas is continuously increasing.

4.3 Carbon emissions

The present ammonia-based chemisorption SSTES-C system was compared to gas boiler and heat pump in terms of carbon emission. The SSTES-C system is charged with solar heat and electricity from April to September, the gas boiler and heat pump are used directly to satisfy the heating demand from October to March. The heating COP (coefficient of performance) of heat pump that was used for calculation and comparison in this work was at 2.5 [30] considering the average ambient temperature of 6 °C from October to March in Newcastle upon Tyne.

The carbon intensities of grid electricity, gas boiler heating and solar heat are presented in Table 3. The carbon intensity of grid electricity in the UK (not including solar electricity) was calculated on half-year basis, from April to September (the non-heating season or energy charging season) and from October to March (the heating season or energy discharging season) respectively, based on the amounts of the electricity generated by fuel types in the year of 2018 (half-hourly data) [31] and the corresponding carbon intensities of different fuels [32]. The carbon intensity of gas boiler heating was considered at 212 gCO_2/kWh given by the work of [33], while that of solar heat was at 10 gCO_2/kWh [34]. It is worth noting that the carbon intensity of electricity generated in summer time is about 16% lower than that in winter due to the higher share of Nuclear power and other renewable energy source in summer.

Based on the data in Table 3, the carbon emissions of different heating technologies are compared in Figure 7 in a range of heating demand studied in this paper. The gas boiler heating which is currently dominating in

the UK yields the highest carbon emission due to its modest efficiency and the usage of non-renewable energy. Electric driven heat pump consumes less energy and achieves the higher energy efficiency, hence its carbon emission is less than that of gas boiler. Since the majority of the energy charged to the system is solar heat and the other part of energy is the summer grid electricity which has the relatively lower carbon intensity, the present SSTES-C system generates the minimum CO_2, about 34.1% and 68.4% of that of gas boiler and heat pump. If solar electricity is used, carbon emission of SSTES-C system can be even lower, only 7.8% and 15.6% of that of gas boiler and heat pump.

Table 3 Carbon intensity of grid electricity, gas boiler heating and solar heat.

April to September grid electricity	222.1 gCO_2/kWh
October to March grid electricity	263.9 gCO_2/kWh
Gas boiler heating [33]	212 gCO_2/kWh
Solar heating [34]	10 gCO_2/kWh

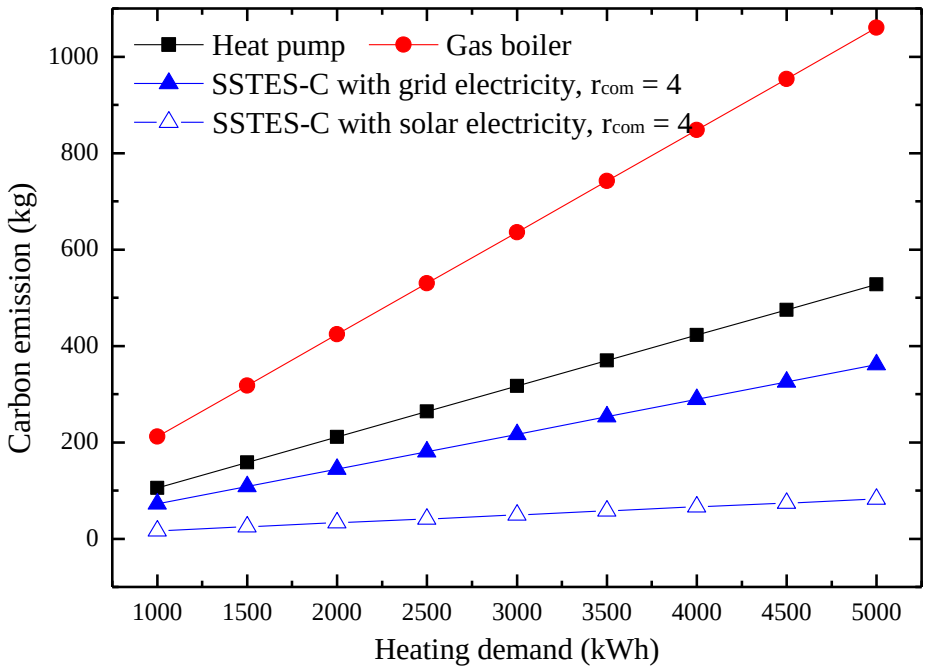

Figure 7 Carbon emissions using SSTES-C system, heat pump and gas boiler.

5 Conclusions

400 The hybrid SSTES system using ammonia chemisorption technology with electricity as supplementary
401 energy source in two different approaches during charging process, through electric heater and compressor,
402 respectively, was investigated and compared in this paper. The major conclusions are:
403 (a) The usage of compressor was significantly more efficient to enhance the storage capacity of the
404 SSTES system. The stored non-loss chemical potential energy could be increased by 2.5~4.3 fold when
405 using a compression ratio of 3~8, compared to only-sorption system.
406 (b) Using electric-driven compressor allowed the ammonia desorption occurred at relatively lower
407 temperature and all the heat input required (including sensible heat and desorption heat) could be supplied by
408 solar heat even in the high latitude city like Newcastle upon Tyne, leading to more solar heat being recovered
409 and stored for heating in the winter.
410 (c) Without electricity input, only 1105 kWh solar heat can be stored over seasons due to the insufficient
411 solar irradiation. By inputting 382-1944 kWh electricity into the SSTES-C system through a compressor
412 which has a compression ratio of 2-8, 733-3208 kWh more solar heat can be recovered to regenerate the
413 SSTES system and 912-3616 kWh (82.5%~327%) more heat can be stored within the studied SSTES-C
414 system. The studied system has the energy density of around 148 kWh/m^3 at the system level. More effort is
415 required to improve the system compactness and heat and mass transfer performance, therefore increasing
416 the system-based energy density closer to the material-based energy density at around 228.68 kWh/m^3.
417 (d) Due to the usage of renewable solar heat and low carbon intensity electricity or solar electricity in
418 summer, the SSTES-C system had noteworthy lower carbon emission compared to widely used gas boiler
419 and heat pump. It was about only 34.1% and 68.4% of that of gas boiler and heat pump if the grid electricity
420 is used, and was only 7.8% and 15.6% if the summer solar electricity is used, e.g. PV/T panel is employed.
421

422 **Acknowledgement**

423 The authors gratefully acknowledge the support from the Heat-STRESS project (EPSRC, EP/N02155X/1)
424 funded by the Engineering and Physical Science Research Council and TRESS project (17754) funded by
425 Innovate UK.
426

427 **Reference**

[1] Department of Business, Energy & Industrial Strategy. Energy consumption in the UK 2018 data tables. 2018. London, UK.

[2] J Xu, RZ Wang, Y Li. A review of available technologies for seasonal thermal energy storage. Solar Energy 2014; 103:610-638.

[3] T Pauschinger. Solar district heating with seasonal thermal energy storage in Germany. Technical Report 2012.

[4] S Himran, A Suwono. Characterization of Alkanes and paraffin waxes for application as phase change energy storage medium. Energy Sources Journal 1994; 16:117-128.

[5] P Pinel, CA Cruickshank, I Beausoleil-Morrison, A Wills. A review of available methods for seasonal storage of solar thermal energy in residential applications. Renewable and Sustainable Energy Review 2011; 15:3341–3359.

[6] N Yu, RZ Wang, LW Wang. Sorption thermal storage for solar energy. Progress in Energy and Combustion Science 2013; 39:489–514.

[7] TX Li, RZ Wang, JK Kiplagat. A target-oriented solid-gas thermochemical sorption heat transformer for integrated energy storage and energy upgrade. AIChE 2013; 59:1334–1347.

[8] L Scapino, HA Zondag, JV Bael, J Diriken, CCM Rindt. Sorption heat storage for long-term low-temperature applications: A review on the advancements at material and prototype scale. Applied Energy 2017; 190:920–948.

[9] D Aydin, SP Casey, S Riffat. The latest advancements on thermochemical heat storage systems. Renewable and Sustainable Energy Review 2015; 41:356–367.

[10] TX Li, RZ Wang, T Yan. Solar-gas thermochemical sorption thermal battery for solar cooling and heating energy storage and heat transformer. Energy 2015; 84:745–758.

[11] N Eyre, P Baruah. Uncertainties in energy demand in residential heating – working paper. UKERC, London, UK, 2014.

[12] NJ Hewitt. Heat pumps and energy storage – the challenges of implementation. Applied Energy 2012; 89: 37–44.

[13] ZW Ma, HB Bao, AP Roskilly. Feasibility study of seasonal solar thermal energy storage in domestic dwellings in the UK. Solar Energy 2018; 162:489–499.

[14] ZW Ma, HB Bao, AP Roskilly. Seasonal solar thermal energy storage using thermochemical sorption in domestic dwellings in the UK. Energy 2019; 166:213–222.

[15] TX Li, RZ Wang, JK Kiplagat, Y Kang. Performance analysis of an integrated energy storage and energy upgrade thermochemical solid-gas sorption system for seasonal storage of solar thermal energy. Energy 2013; 50:454–467.

[16] TX Li, S Wu, T Yan, RZ Wang, J Zhu. Experimental investigation on a dual-mode thermochemical sorption energy storage system. Energy 2017; 140:383–394.

[17] L Jiang, RZ Wang, LW Wang, AP Roskilly. Investigation on an innovative resorption system for seasonal thermal energy storage. Energy Conversion and Management 2017; 149:129–139.

[18] Ph Touzain. Thermodynamic values of ammonia salts reaction for chemical sorption heat pumps. Proceedings of the international sorption heat pump 1999, Munich, Germany.

[19] P Donkers, L Pel, M Steiger, O Adan. Deammoniation and ammonia processes with ammonia complexes. AIME Energy 2016; 4:936–950.

[20] RG Oliveira, RZ Wang, JK Kiplagat, CJ Chen. NaBr-expanded graphite consolidated sorbent for low temperature driven chemisorption air conditioner. International sorption heat pump conference 2008, Seoul, Korea.

[21] RZ Wang, LW Wang, JY Wu. Adsorption refrigeration technology - Theory and application. Wiley 2014.

[22] Johannessen T. 3rd generation SCR system using solid ammonia storage and direct gas dosing: - Expanding the SCR window for RDE. In: Directions in Engine Efficiency and Emissions Research (DEER) Conference, Dearborn, Michigan, US, 2012.

[23] HS Bao, ZW Ma, AP Roskilly. Chemisorption power generation driven by low grade heat – Theoretical analysis and comparison with pumpless ORC. Applied Energy 2017; 186: 282–290.

[24] S Wu, TX Li, T Yan, RZ Wang. Experimental investigation on a thermochemical sorption refrigeration prototype using EG/$SrCl_2$–NH_3 working pair. International Journal of Refrigeration 2018; 88:8–15.

[25] K Thinsurat, HS Bao, ZW Ma, AP Roskilly. Performance study of solar photovoltaic-thermal collector for domestic hot water use and thermochemical sorption seasonal storage. Energy Conversion and Management 2019; 180:1068–1084.

485 [26] HJ Huang, GB Wu, J Yang, YC Dai, WK Yuan, HB Lu, Modeling of gas-solid chemisorption in
486 chemical heat pumps, Sep. Purif. Technol. 2004; 34:191–200.
487 [27] Y Yuan, HS Bao, ZW Ma, YJ Lu, AP Roskilly. Investigation of equilibrium and dynamic
488 performance of SrCl2-expanded graphite composite in chemisorption refrigeration system. Applied Thermal
489 Engineering 2019, 147:52–60.
490 [28] Energy Saving Trust. Solar energy calculator sizing guide. 2015.
491 http://www.pvfitcalculator.energysavingtrust.org.uk/Documents/150224_SolarEnergy_Calculator_Sizing_G
492 uide_v1.pdf. [Accessed 20 June 2018].
493 [29] JP Zimmermann, M Evans, J Griggs, N King, L Harding, P Roberts, C Evans. Household electricity
494 survey A study of domestic electrical product usage. Intertek Report R66141.
495 [30] I Staffell, D Brett, N Brandon, A Hawkes. A review of domestic heat pumps. Energy and
496 Environmental Science 2012; 5:9291–9306.
497 [31] https://www.bmreports.com/bmrs/?q=generation/fueltype
498 [32] I Staffell. Measuring the progress and impacts of decarbonising British electricity. Energy Policy
499 2017; 102:463–475.
500 [33] C Pout. Proposed carbon emission factors and primary energy factors for SAP 2012. BRE, editor.
501 Technical papers Supporting SAP (2012).
502 [34] The Parliamentary Office of Science and Technology. Carbon footprint of heat generation.
503 POSTNOTE 2016, 523, London UK.